Macromolecules **1995,** *28,* 7869−7878 **7869**

Topological Effects on Blend Miscibility

W. L. Nachlis,[†,‡] **J. T. Bendler,***[†,§] **R. P. Kambour,**[†] **and W. J. MacKnight**[‡]

General Electric Corporate Research and Development, Schenectady, New York 12301, and Polymer Science and Engineering Department, University of Massachusetts, Amherst, Massachusetts 01003

Received July 25, 1994; Revised Manuscript Received August 15, 1995[⊗]

ABSTRACT: The thermodynamics of mixing is shown to be quite sensitive to changes in the topology of blend components. Cyclic Bisphenol A carbonate oligomers are miscible with a wider range of polystyrene (PS) molecular weights than are chemically equivalent linear oligomers. The Flory−Huggins mean-field theory predicts the shape of phase boundaries quite well for linear PS/linear polycarbonate (PC) blends as well as for linear PS/cyclic PC blends. However, the interaction parameter is strongly dependent upon topology with $\chi_{PS_L/PC_C} < \chi_{PS_L/PC_L}$. This result is explained in terms of a topological repulsion between rings, which is expected to be quite general.

Introduction

The ability of polymer chemists to synthesize topologically unique polymer molecules has stimulated great interest in the properties of block-, star-, and ring-shaped polymers. The viscoelastic, hydrodynamic, and diffusion characteristics of cyclic polymers have been of particular interest, providing novel systems with which to validate established theories such as reptation.[1−6] The objective of the present work is to investigate the influence of topology on the thermodynamics of mixing. While the equilibrium thermodynamic properties of blends of linear polymers continue to be the subject of great commercial and academic interest,[7−10] the effect of topological variations in blend components has only recently been considered.[11,12]

The thermodynamic stability of blends of 22-arm star polystyrene with linear poly(vinyl methyl ether) (PVME) has been compared to that of linear/linear blends of equivalent molecular weight.[12] LCST behavior was observed for both the star/linear and linear/linear blends. Although, the temperature minima of cloud point curves were found to be the same for both cases, a small compositional shift toward the star-rich portion was observed. This shift was attributed to star-core exclusion resulting from the high functionality of the branch point. A region of very high segment density exists at the core of the 22-arm star which in effect shields the core from interactions with other molecules causing the shift in composition.

Santore et al. compared the phase separation behavior of blends of cyclic polystyrene with linear PVME to that of linear/linear blends of equivalent molecular weight.[11] Cyclic/linear blends exhibited LCST behavior as observed for linear/linear blends. However, in contrast to star/linear blends, cloud point curves for cyclic/linear systems were shifted only in temperature and not in composition. The cloud points for cyclic/linear blends were 7−8 °C higher than those for linear/linear systems over the composition range from 10 to 65 wt % polystyrene. Thus, cyclic polystyrene/linear PVME blends display a wider temperature range of thermodynamic stability than equivalent linear/linear systems. Although this enhanced stability has not been predicted by any theory, Cates and Deutsch conjectured that blends of chemically identical cyclics and linears should display a negative Flory−Huggins χ parameter and that an extension of that logic suggests that chemically dissimilar ring/linear combinations might be miscible in cases where linear/linear combinations are immiscible.[13] It was also noted that the observed enhanced stability of cyclic/linear blends could be rationalized in terms of changes in the free energy of one pure component of a blend due to cyclization.[11]

The effect of topological variations in blend components will be addressed in the present work by comparing the miscibility of Bisphenol A carbonate cyclic oligomers (BPACY) as well as that of equivalent linear oligomers with a variety of linear polymers. The synthesis of BPACY as well as their ring-opening polymerization to form high molecular weight polycarbonate has recently been reported by Brunelle et al.[14−16] The majority of the work reported here involves the miscibility of cyclic and linear Bisphenol A carbonate oligomers with a series of narrow molecular weight distribution polystyrenes. The determination of the critical polystyrene molecular weight for complete miscibility allowed the Flory−Huggins χ parameter for linear carbonate oligomer/polystyrene blends as well as cyclic carbonate oligomer/polystyrene blends to be determined.

Experimental Section

Unless otherwise noted, reagent grade solvents and chemicals were used without further purification. The synthesis of BPACY has been described elsewhere and is outlined in Figure 1.[14−16] The BPACY used in this study were provided by General Electric Corporate Research and Development. The as-received BPACY were fractionated by Soxhlet extraction with refluxing heptane over a period of 9 days. This yielded a low molecular weight fraction (BPACY-LF), soluble in refluxing heptane, as well as high molecular weight fraction (BPACY-HF) insoluble in heptane.

The molecular weight of the three BPACY samples were determined by HPLC analysis using a Perkin-Elmer HPLC system comprised of a Model 410 pump, ISS-100 autoinjector, and LC-235 diode array detector. These components were interfaced with a Nelson Analytical Model 2600 chromatography data station used for data reduction. A C-8 reversed-phase column was used with a THF/water gradient. The gradient used was as follows: solvent A, 30% THF/water; solvent B, THF. (Step 1) 40−75% B over 15 min. at exponent −2; (step 2) 75−100% B over 3 min at exponent −1; (step 3) 100% B for 4 min; (step 4) 100−40% B over 2 min (recycle). Complete absolute molecular weight distributions and averages were calculated from relative peak areas directly since

---

[*] Author to whom correspondence should be addressed.

[†] General Electric Corporate Research and Development.

[‡] University of Massachusetts.

[§] Present address: Department of Chemistry & Chemical Engineering, South Dakota School of Mines & Technology, Rapid City, SD 57701.

[⊗] Abstract published in *Advance ACS Abstracts,* October 15, 1995.

0024-9297/95/2228-7869$09.00/0

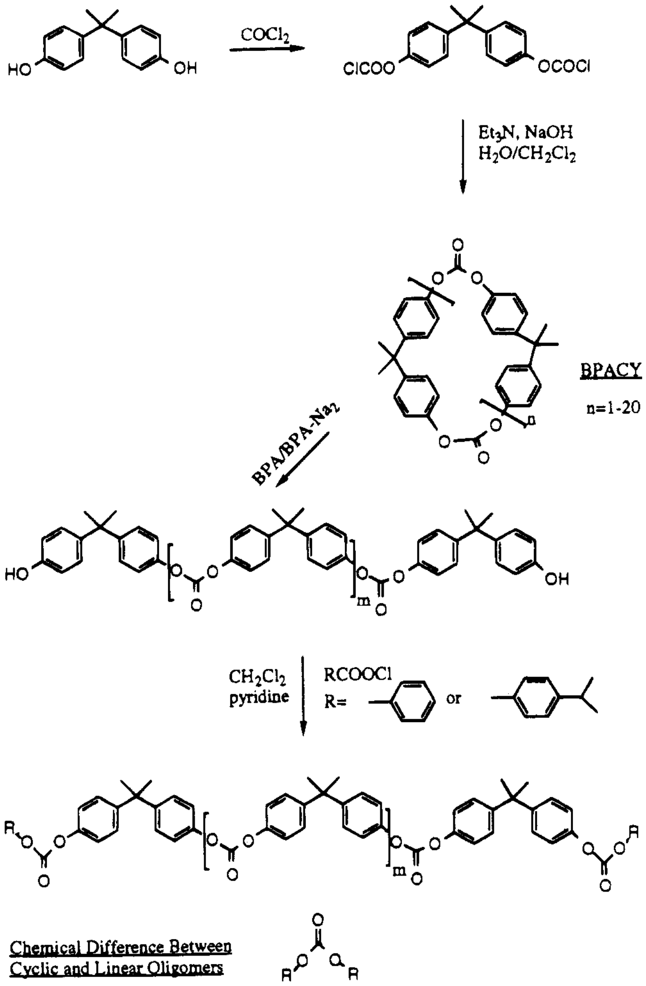

Figure 1. Preparation of cyclic and linear Bisphenol A carbonate oligomers.

Table 1. Cyclic and Linear Carbonate Oligomers

	T_g (°C)	density (g/mL)	M_n (NMR)	M_n (LC)	M_w	M_z
BPACY	147	1.197 ± 0.001		1144	1529	2228
BPACY-HF	146	1.196		1493	1987	2783
BPACY-LF	136	1.197		876	997	1140
PCLN	82	1.214	1501	1558	2074	2716
PCLN-LF	70	1.215	1350	1195	1367	1518
IPLN	73	1.183	1406	1012	2182	3106
IPLN-LF	70	1.181	1518	1193	1803	2050

relative response factors are independent of oligomer molecular weight.[17] The results of these calculations are presented in Table 1. As isolated, the BPACY have a $T_g = 147$ °C as well as a significant degree of crystallinity ($T_m = 200-210$ °C) and contain less than 0.05% linear contaminants. Completely amorphous BPACY can be obtained by solution casting from hot *o*-dichlorobenzene at ~160 °C. Densities of completely amorphous samples were determined by flotation in aqueous magnesium sulfate solutions (see Table 1).

Linear Bisphenol A carbonate polymers were prepared by solution equilibration of BPACY with a Bisphenol A (BPA)/Bisphenol A disodium salt (BPA-Na_2) mixture. In a typical preparation, BPACY (100 g, 0.393 mol) were dissolved in 750 mL of methylene chloride in a 1-L round-bottom flask to which were added BPA (22.2 g, 0.0973 mol) and BPA-Na_2 (0.268 g, 0.983 mmol). The flask was then fitted with a condenser and refluxed for 2 h. Hydroxyl-capped linear oligomers were isolated by precipitation in methanol (see Figure 1).

These crude linear oligomers are chemically quite different from the BPACY due to the presence of the hydroxyl end group. Therefore, the hydroxyl end groups were converted to aryl carbonates via reaction with an appropriate aryl chloroformate. Two different chloroformates were used, phenyl chloroformate and 4-isopropylphenyl chloroformate. This yielded diphenyl carbonate end-capped linear oligomers (PCLN) as well as di-(4-isopropyl)phenyl carbonate-capped linear oligomers (IPLN). End capping was accomplished by dissolving the hydroxyl-capped linear oligomers (10 g, 39 mmol) and pyridine (3.6 g, 40 mmol) in 100 mL of methylene chloride. This solution was cooled to 0 °C. A solution of the appropriate aryl chloroformate (40 mmol in 100 mL of methylene chloride) was then added slowly over 30 min, while stirring magnetically. After an additional 30 min, 15 mL of water was added and stirring continued for another 15 min. The solution of capped linear oligomers was washed twice with 3 N HCl, twice with 2 M NaOH, and finally with water. After being dried over $MgSO_4$ and filtered, the solution was evaporated to yield aryl carbonate-capped linear oligomers (see Figure 1). ^1H NMR spectra, obtained in CD_2Cl_2 using a GE QE-300 spectrometer, revealed that the end-capping procedure was extremely efficient. A resonance at 6.7 ppm due to aromatic protons ortho to a hydroxyl end group is observed only in the uncapped linear spectrum and is completely absent in the spectra of capped linears. HPLC analysis confirmed the absence of hydroxyl end groups.

The linear oligomers were fractionated in order to obtain fractions with slightly lower average molecular weights. Fractionation was accomplished by dissolving the capped oligomers in toluene (10 g of oligomers/100 mL of toluene) and adding heptane (26 mL). The highest molecular weight oligomers are least soluble in the toluene/heptane mixture and therefore were preferentially precipitated. The low molecular weight fractions were isolated by filtration and evaporation of the supernatant. This yielded the respective low molecular linear fractions PCLN-LF and IPLN-LF. Absolute molecular weights were determined via HPLC analysis by employing the same procedure used for BPACY as well as from ^1H NMR data. Molecular weights, T_g's, and amorphous glass densities, determined as above for BPACY, are given in Table 1.

The T_g's of the cyclic oligomers are significantly higher than those of linear oligomers of similar molecular weight. This phenomenon has been observed in several other ring systems and has been explained in terms of the lower configurational entropy of glasses of ring polymers relative to that of linears.[18] Although T_g usually increases with decreasing molecular weight for ring systems, the slight reduction in T_g for BPACY-LF can be explained in terms of a large increase in intramolecular stiffness for the smaller rings.[18]

Blends of cyclic and linear Bisphenol A carbonate oligomers with various chemically dissimilar linear polymers were prepared via solution casting. Blend components were dissolved in hot *o*-dichlorobenzene (0.01 wt % Ultranox 626, GE Specialty Chemicals, added as antioxidant) and cast onto a glass Petri dish which has been treated with chlorotrimethylsilane. Films were cast at 165 °C in order to prevent crystallization of the carbonate oligomers. Films were dried under vacuum (slight N_2 purge) at temperatures between 130 and 160 °C, depending upon the T_g's of components, for at least 3 days. Thermal gravimetric analysis (Perkin-Elmer TGA-7) confirmed complete removal of casting solvent. Blend T_g's were determined using a Perkin-Elmer DSC-7 at a heating rate of 20 °C/min. All samples were held at 200 °C for 5 min in the DSC and quenched prior to analysis. Thermodynamic equilibrium was assumed to have been reached during this 5-min hold at 200 °C. The one-phase/two-phase boundary was then determined from the T_g measurements. Miscibility (i.e., a composition in the one-phase region) was judged based on the appearance of a single T_g. Blends containing BPACY were analyzed by GPC to ensure that no polymerization occurred during thermal treatment.

Results and Discussion

Miscibility of BPACY with Various Linear Polymers. The investigation of the miscibility of BPACY with various linear polymers began by determination of the phase behavior of 50/50 wt % blends of the cyclic oligomers with polymers spanning a range of cohesive

Table 2. Polymers Used in Blending Studies and Results for 50/50 BPACY/Polymer Blends

polymer	source	CED[a] (J/cm^3)	T_g (°C)	50/50 wt % BPACY/Polymer T_g (°C)
BPA polyformal[19] $[\eta]CHCl_3$ = 0.5 dL/g	GE CRD	318	90	108
poly(2,6-dimethylphenylene oxide) $[\eta]_{CHCl_3}$ = 0.49 dL/g	GE CRD	339	214	180
polystyrene[b]	Pressure Chemical	339		
PS(1.5K)	Pressure Chemical	339	45	84
PS(2.5K)	Pressure Chemical	339	66	97
PS(4K)	Pressure Chemical	339	78	103
PS(10K)	Pressure Chemical	339	95	115
PS(20.4K)	Pressure Chemical	339	101	119
PS(31.5K)	Pressure Chemical	339	98	118
PS(51K)	Pressure Chemical	339	105	119, 149
PS(100K)	Pressure Chemical	339	105	119, 145
PS(160K)	Pressure Chemical	339	106	118, 147
PS(670K)	Pressure Chemical	339	108	121, 149
poly(methyl methacrylate) (M_w = 93K)	Scientific Polymer Products	377	100	127
poly(vinyl acetate)	Aldrich Chem. (Catalog No. 18948-0)	377	31	91
poly(vinyl chloride)	Polysciences (Catalog No. 2776)	377	80	113
styrene–acrylonitrile copolymers				
16% AN (M_w = 110K)	B. Schmidt, BASF, Germany	375	107	124
30% AN (M_w = 56K)	B. Schmidt, BASF, Germany	406	106	124
35% AN (M_w = 130K)	B. Schmidt, BASF, Germany	418	109	124
poly(ether sulfone)[c] Victrex grade 200P	ICI	490	230	178
poly(phenyl sulfone)[c] Radel resin	Union Carbide	527	213	177

[a] Kambour, R. P. *Polym. Commun.* **1983**, *24*, 292. [b] Narrow molecular weight distribution polystyrene standard ($M_w/M_n \le 1.06$). Molecular weight given in parentheses (100 000 = 100K). [c] Cast from dimethylacetamide (165 °C).

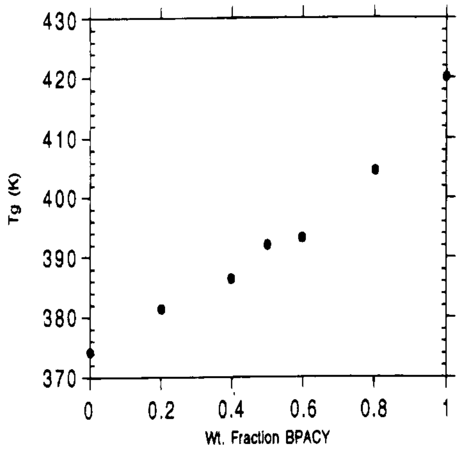

Figure 2. T_g vs composition BPACY/PS(20.4K) blends.

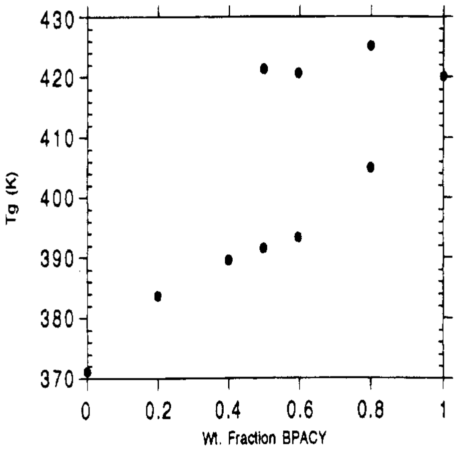

Figure 3. T_g vs BPACY/PS(31.5K) blends.

energy densities (CEDs). The results of this survey are presented in Table 2. A surprising number of these blends are single phase, as judged by a single T_g. BPACY are miscible with relatively nonpolar polymers such as BPA polyformal (CED = 318 J/cm^{3-}) as well as more polar polymers including poly(phenylsulfone) (CED = 537 J/cm^3). The BPACY were found to be immiscible only with polystyrenes of molecular weight greater than 20 400.

Miscibility of BPACY with Polystyrene. The observation of a miscibility gap in terms of polystyrene molecular weight enables the determination of the Flory–Huggins χ parameter, which will be discussed later. Therefore, in order to more completely describe the miscibility of BPACY with polystyrene, blends of BPACY and polystyrenes of molecular weights between 1.5K and 670K, of varying composition, were prepared and analyzed by DSC.

BPACY are miscible at all compositions with polystyrenes of molecular weight less than 20.4K. T_g vs composition is shown in Figure 2. Phase separation occurs at BPACY compositions greater than 40 wt % for blends with PS(31.5K) (see Figure 3). Similar behavior is observed for blends of BPACY with PS(51K) and PS(100K). Blends of BPACY with PS(160K) as well as PS(670K) phase separate at compositions greater than 20 wt % BPACY. These results are summarized in Figure 4.

The T_g composition behavior of phase-separated systems reveals that when phase separation occurs one phase is essentially pure BPACY while the composition of the PS-rich phase is dependent on the overall blend composition. In all cases, the polystyrene-rich phase contains more BPACY at higher contents of BPACY in the blend. For example, the T_g of the PS-rich phase in a 50/50 blend of BPACY/PS(31.5K) is lower than that of the PS-rich phase of a 80/20 blend. The significance of this will be discussed later.

Similar results were obtained for blends of BPACY-HF with the various molecular weight polystyrenes. As expected, the critical polystyrene molecular weight for miscibility is lower for this higher molecular weight

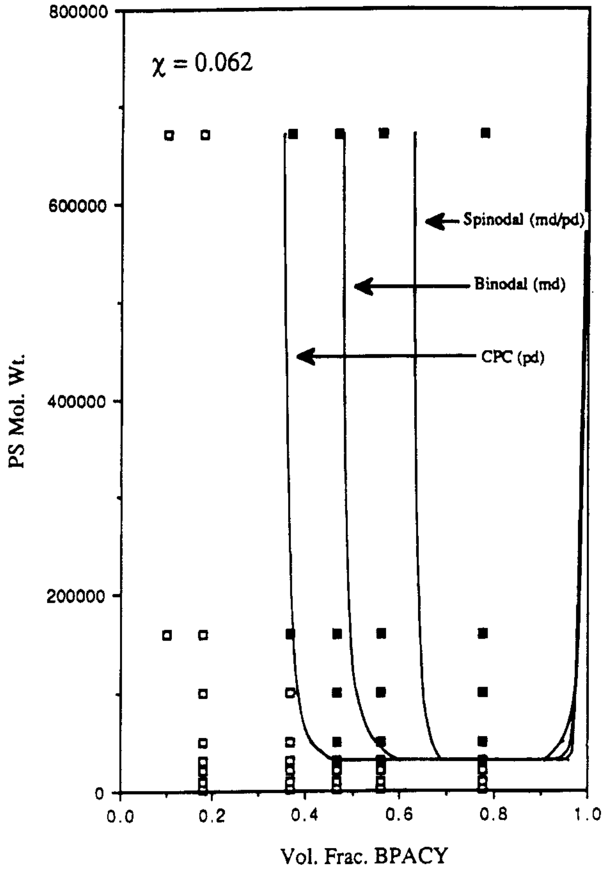

Figure 4. Experimental and Flory–Huggins predicted phase boundaries for blends of BPACY/PS (χ = 0.062; see text). Experimental data: open squares, miscible blends, single T_g; closed squares, immiscible blends, two T_g's. The experimental points assume that thermodynamic equilibrium was obtained after holding the blend for 5 min at 200 °C.

fraction of cyclic oligomers. BPACY-HF are miscible at all compositions with PS(4K) but form immiscible blends with PS(10K) at compositions between 20 and 80 vol % BPACY-HF (see Figure 5). The low molecular weight fraction of cyclic oligomers, BPACY-LF, were found to be miscible with PS(20.4K) at all compositions and immiscible with PS(51K) for BPACY-LF compositions greater than 50 wt %.

Miscibility of Linear Oligomers with Polystyrene. The miscibilities of Bisphenol A carbonate linear oligomers, PCLN, PCLN-LF, IPLN, and IPLN-LF, with various molecular weight polystyrenes were also characterized in order to complete the investigation of the topological effects on miscibility. The PCLN were found to be immiscible with the lowest molecular weight polystyrene we had available, PS(1.5K). However, the lower molecular weight fraction, PCLN-LF, was miscible with PS(1.5K) at all compositions but immiscible with PS(2.5K) at 50 wt % PCLN-LF. Similarly, the IPLN were determined to be immiscible with the lowest available polystyrene. The lower molecular weight fraction, IPLN-LF, was found miscible with PS(1.5K) across the composition range but immiscible with PS-(2.5K) at 50 wt % (see Figure 6). The critical polystyrene molecular weight data for miscibility for all oligomers investigated are summarized in Table 3.

Determination of Flory–Huggins χ Parameter. Qualitatively, the cyclic carbonate oligomers are significantly more miscible with polystyrene than are the equivalent linear oligomers. The critical polystyrene molecular weight for the highest molecular weight cyclic fraction, BPACY-HF (M_w = 1987), is between 4K and 10K while that for both the lower molecular weight linear fractions PCLN-LF (M_w = 1367) and IPLN-LF (M_w = 1803) is between 1.5K and 2.5K. Application of FLory–Huggins solution theory will enable a more quantitative evaluation of the topological effects on the thermodynamics of mixing.

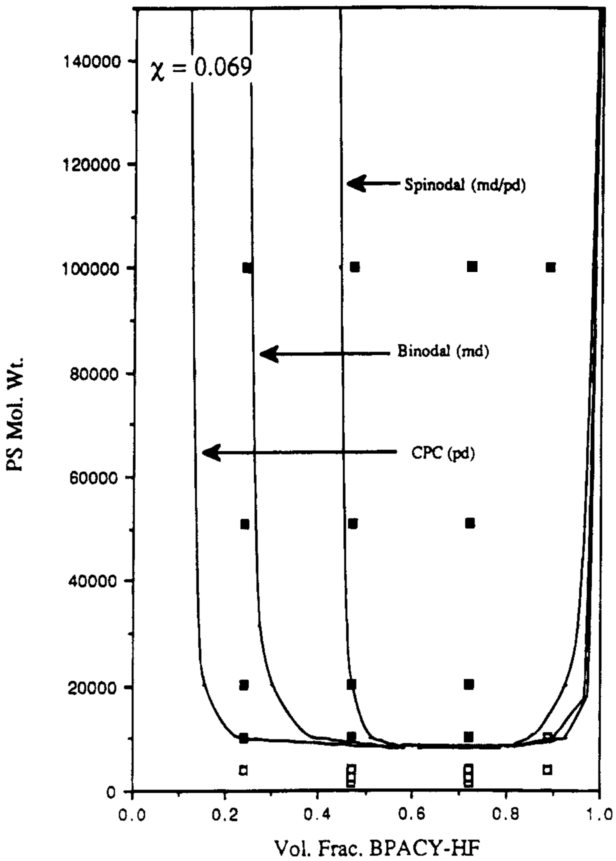

Figure 5. Experimental and Flory–Huggins predicted phase boundaries for blends of BPACY-HF/PS (χ = 0.069; see text). Experimental data: open squares, miscible blends, single T_g; closed squares, immiscible blends, two T_g's.

Flory–Huggins solution theory gives the following expression for the free energy of mixing for a quasi-binary system in which one or both components are polydisperse[20–24]

$$\frac{\Delta G_m}{RT}\left(\sum_i \frac{\phi_{1i}}{N_{1i}} \ln \phi_{1i} + \sum_j \frac{\phi_{2j}}{N_{2j}} \ln \phi_{2j}\right) + \chi_{12}\phi_1\phi_2 \quad (1)$$

where R is the gas constant and ϕ_i and N_i are the volume fraction and degree of polymerization of species i, respectively. The N_i's are given in terms of a reference segment volume, V_{ref}, which is usually taken as the smaller of the two repeat unit volumes. The combinatorial entropy of mixing is given by the term in parentheses. In the original derivation, the second term on the right-hand side represented the enthalpy of mixing. It has since been generalized to include noncombinatorial entropic effects.[25] χ_{12} is defined as

$$\chi_{12} = -\frac{\Delta w_{12} V_{ref}}{RT} \quad (2)$$

Thus Δw_{12} represents the local free energy change per unit volume for the process of exchanging unlike contacts for like contacts

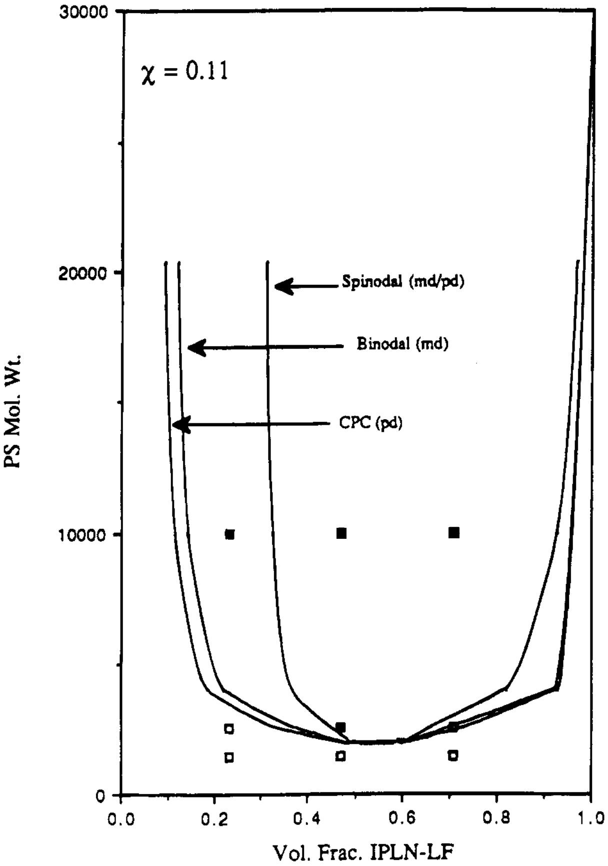

Figure 6. Experimental and Flory–Huggins predicted phase boundaries for blends of IPLN-LF/PS (χ = 0.11; see text). Experimental data: open squares, miscible blends, single T_g; closed squares, immiscible blends, two T_g's.

$$2[12] \Leftrightarrow [11] + [22] \tag{3}$$

$$\Delta w_{12} = w_{11} + w_{22} - 2w_{12} \tag{4}$$

The average segmental potentials between like segments given by w_{ii} and that between unlike segments by w_{ij}. Therefore, Δw_{12} represents all local enthalpic and entropic effects related to breaking like contacts and forming unlike contacts, with χ_{12} now becoming an empirical parameter representing the excess free energy of mixing. When $\Delta w_{12} > 0$, unlike contacts are favored, $\chi_{12} < 0$, and mixing is favored. Conversely, when $\Delta w_{12} < 0$, like contacts are favored, $\chi_{12} > 0$, and demixing is favored. χ_{12} has been found to be dependent upon concentration and molecular weight also in contradiction with its original interpretation.[26] In this work, the potential dependence of χ_{12} on composition and molecular weight will be neglected.

A simple physical explanation for this mixing "law" for polymer mixtures has been given by Flory.[27] Basically, the combinatorial entropy of mixing is due to the greater volume over which the molecules of both components are distributed in a mixture relative to the pure components. Flory has also shown that within the framework of this model the combinatorial entropy is independent of the average configuration of the polymeric components. Thus, the treatment is equally applicable to mixtures of linear polymers and ring- or rod-shaped molecules.[27]

Given an expression for the free energy of mixing (eq 1), complete phase boundaries (i.e., binodals and spinodals for binary systems and cloud point curves, shadow curves and spinodals for quasi-binary systems) can be determined in terms of N_i, N_j, ϕ_i, and χ_{ij}. The critical condition for any binary or pseudo-binary system is given by simultaneous solution of the spinodal condition

Table 3. Critical Polystyrene Molecular Weights for Miscibility and Calculated Interaction Parameters

	miscible	immiscible	χ_{PS_L/PC_C} or χ_{PS_L/PC_L}
BPACY	PS(20.4K)	PS(31.5K)	$0.057 < \chi_{PS_L/PC_C} < 0.062$
BPACY-LF	PS(20.4K)	PS(51K)	$0.076 < \chi_{PS_L/PC_C} < 0.087$
BPACY-HF	PS(4K)	PS(10K)	$0.074 < \chi_{PS_L/PC_C} < 0.076$
PCLN		PS(1.475K)	$0.13 < \chi_{PS_L/PC_L}$
PCLN-LF	PS(1.475K)	PS(2.5K)	$0.13 < \chi_{PS_L/PC_L} < 0.16$
IPLN		PS(1.475K)	$0.12 < \chi_{PS_L/PC_L}$
IPLN-LF	PS(1.475K)	PS(2.5K)	$0.11 < \chi_{PS_L/PC_L} < 0.14$

$$(\partial^2 \Delta G / \partial \phi_2^{\,2})_{P,T} = 0 \tag{5}$$

and

$$(\partial^3 \Delta G / \partial \phi_2^{\,3})_{P,T} = 0 \tag{6}$$

which yields[26–30]

$$\chi_{\text{crit}} = \frac{1}{2}\left(\frac{1 + \sqrt{a_2 N_{w_1} / a_1 N_{w_2}}}{N_{w_1}} + \frac{1 + \sqrt{a_1 N_{w_2} / a_2 N_{w_1}}}{\mathrm{N}_{w_2}}\right) \tag{7}$$

with

$$a_i = M_{zi}/M_{wi} \tag{8}$$

Here N_{wi} is the weight-average degree of polymerization in terms of V_{ref}, and M_{zi} and M_{wi} are the respective *z*-average and weight-average molecular weights. Flory–Huggins solution theory results in χ_{ij} at the critical point being a simple function of the components' molecular weight distributions.

The experimental observation of a miscibility gap in terms of polystyrene molecular weight (Table 3) can now be used with eqs 7 and 8 to put bounds on χ_{ij} for both linear polystyrene/cyclic polycarbonate, χ_{PS_L/PC_C}, and linear polystyrene/linear polycarbonate, χ_{PS_L/PC_L}. Degrees of polymerization are defined in terms of the molar volume of a polystyrene repeat unit, V_{ref} = 99.6 mL/mol, which is roughly half that of a Bisphenol A carbonate repeat unit, since V_{BPAPC} = 212 mL/mol. The results of these calculations are given in Table 3. We find that the χ parameter for linear polystyrene/cyclic polycarbonate blends, χ_{PS_L/PC_C}, is significantly lower than that for linear polystyrene/linear polycarbonate, χ_{PS_L/PC_L}. A rationalization for this behavior will be presented later.

The χ parameters calculated above in conjunction with detailed knowledge of the molecular weight distributions of blend components enabled the calculation of complete phase boundaries given an expression for the free energy of mixing (eq 1). Phase boundaries were calculated for both truly binary mixtures (i.e., both components monodisperse) and the pseudobinary case (i.e., assume polystyrene monodisperse but account for the dispersivity in carbonate oligomer molecular weight). The precise experimental molecular weight distributions obtained via HPLC for the carbonate oligomers were used in pseudobinary calculations. In all cases, the interaction parameter was assumed independent of composition and molecular weight.

Binodals were calculated for the truly binary case by applying the equilibrium condition

$$\Delta(\mu_1)_A = \Delta(\mu_1)_B \text{ and } \Delta(\mu_2)_A = \Delta(\mu_2)_B \qquad (9)$$

The chemical potential of a component must the same in both phases at equilibrium. Where

$$\Delta\mu_i = \frac{\partial\Delta G}{\partial n_i}\Big|_{P,T,n_j} \qquad (10)$$

Application of these conditions to eq 1 leads to a system of equations that can be solved numerically. In this work computational results were obtained using software programs from Biosym Technologies of San Diego.[28]

In binary systems, the binodal represents three coincident curves: (1) The locus of cloud points; (2) the locus of incipient phases coexisting with the principle phases; (3) the locus of two coexisting "macrophases" which develop as the temperature (or χ) moves beyond the cloud point.

In quasi-binary systems, the binodal still exists but as a multidimensional hypersurface in temperature– (or χ–) composition space instead of the more familiar two-dimensional curve. Further, instead of the three curves listed above being coincident with a two-dimensional binodal, each curve has a unique two-dimensional projection in temperature–composition space. These projections are not generally coincident. Thus, there exist three separate curves representing (1) the locus of cloud points (cloud point curve); (2) the locus of incipient phases coexisting with corresponding principle phases (shadow curve); (3) the locus of coexisting phases as temperature (i.e., χ) is changed (coexistence curve). The Biosym software also provided algorithms for the determination of these curves as well as spinodals employing methods described by others previously.[20–24,28]

The calculated phase boundary for BPACY/PS(20.4K) blends is shown in Figure 7. The effects of polydispersity are quite dramatic. The cloud point curve for the pseudobinary is skewed relative to the binodal calculated by assuming monodisperse components. In addition, the critical point has shifted down the right branch of the spinodal toward higher BPACY compositions. Note also the shift in the shadow curve relative to the cloud point curve. The spinodal for the pseudobinary case is coincident with that for the monodisperse case since the weight-average degree of polymerization of BPACY was used for monodisperse calculations. The corresponding phase boundary for BPACY/PS(31.5K) is shown in Figure 8.

The compositions at the binodals (assuming both components are monodisperse), spinodals, and cloud point curves for a particular value of the interaction parameter were obtained via calculations of this type for the range of polystyrene molecular weights studied. The results for $\chi_{PS_L/PC_C} = 0.062$ are summarized in Figure 4. The chosen value of χ_{PS_L/PC_C} was based on the results given in Table 3. Similar results for BPACY-HF/polystyrene blends as well as IPLN-LF/polystyrene blends are shown in Figures 5 and 6. In all cases, the Flory–Huggins cloud point curves calculated by using an interaction parameter estimated from critical molecular weight data represent the experimental phase boundaries very well. The calculated spinodals and monodisperse binodals are far too narrow. With proper consideration of polydispersity, the mean-field Flory–Huggins theory predicts the shape of the phase boundary quite well for both cyclic/linear blends and linear/linear blends. These results also demonstrate the errors involved in interpreting partial miscibility in terms of spinodal criteria, as is often done in the literature due to the difficulty in calculating binodals and cloud point curves.

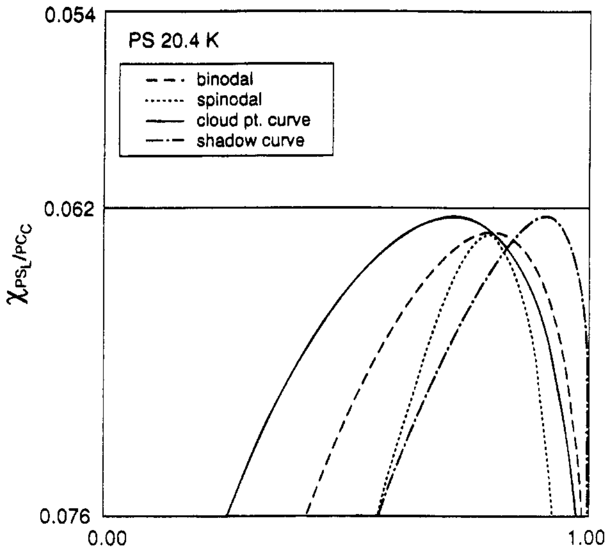

Figure 7. Calculated phase boundary for BPACY/PS(20.4K). (Note that χ increases from top to bottom.)

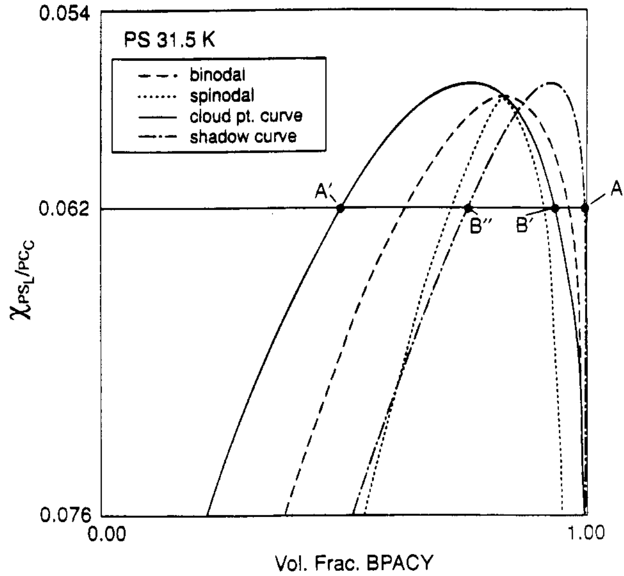

Figure 8. Calculated phase boundary for BPACY/PS(31.5K). (Note that χ increases from top to bottom.)

The calculation of the pseudobinary phase boundaries also yields an explanation for the dependence of the composition of the polystyrene-rich phase on the overall blend composition. In truly binary systems (i.e., monodisperse) with a composition independent χ, a horizontal tie line can be drawn connecting two points on the binodal. These two points represent equilibrium-phase compositions at a particular value of the interaction parameter (or temperature). Further, these two compositions are coupled; when one represents the principal phase the other represents the incipient phase and vice versa. In contrast, a simple horizontal tie line cannot be drawn if either of the components is polydisperse since, as discussed above, the binodal can no longer be represented as a simple two-dimensional curve. Instead, it is essential to realize that coupled to the cloud point curve, representing the locus of principal phases,

Table 4. Solubility Parameters of Polymers and End Groups

structure	δ (cal/mL)$^{1/2}$
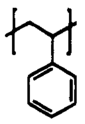	9.0[a]
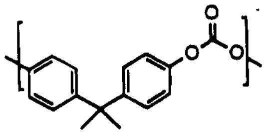	10.4[a]
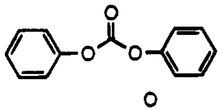	11.5[b]
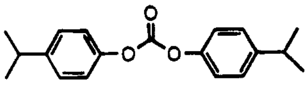	10.1[b]

[a] Van Krevelen, D. W. *Properties of Polymers*; Elsevier: New York, 1976. [b] Estimated by group contribution methods given by Van Krevelen (footnote *a*).

is the shadow curve representing the locus of incipient phases. These curves are generally not coincident when the components are polydisperse.

For example, for blends of BPACY with PS(31.5K) ($\chi_{PS_L/PC_C} = 0.062$), when the volume fraction of BPACY in the principal phase is 0.46 (A′, Figure 8) the shadow curve reveals that the incipient phase is pure BPACY (A″, Figure 8). However, when the volume fraction of BPACY in the principal phase is 0.94 (B′, Figure 8), the incipient phase is 73% BPACY (B″, Figure 8). We see that polydispersity breaks the coupling of incipient phase compositions; this uncoupling explains the dependence of equilibrium phase compositions on the overall blend composition.

Two other studies have given values for χ_{PS_L/PC_C}. Kim and Burns[29] determined $\chi_{PS_L/PC_L} = 0.038$ at 250 °C (polycarbonate segment used as V_{ref}, 212 mL/mol), which corresponds to $\chi_{PS_L/PC_C} = 0.018$ if V_{ref} is a polystyrene segment (99.6 mL/mol). Equilibrium phase compositions were estimated from T_g shifts using high molecular weight polymers with large polydispersities ($M_w/M_n > 2.3$). This value is in poor agreement with that found in this work and actually predicts complete miscibility for many of the systems found only partially miscible. The assumptions made in their work concerning phase compositions and polydispersity are quite different from the treatment given here and may well be the source of the discrepancy. Callaghan and Paul also investigated this system.[30] Their value for χ_{PS_L/PC_C} is also in poor agreement, which may be due to their interpretation of partial miscibility using spinodal criteria.

As noted in Figure 1, the chemical difference between a linear oligomer and a cyclic due to the presence of end groups is only the addition of a diaryl carbonate. We have attempted to keep the end groups as chemically similar to bisphenol A carbonate as possible and, further, have investigated two different end groups. The chemical nature of the end groups relative to polystyrene and Bisphenol A polycarbonate can be interpreted in terms of their solubility parameters (see Table 4). The solubility parameter for diphenyl carbonate is higher than that for both polystyrene and polycarbonate. Therefore, we would expect the presence of this end group to result in slightly decreased miscibility. Diisopropylphenyl carbonate has a solubility parameter that lies between that of polycarbonate and polystyrene; in this case, we would expect the presence of the end group to make the linear oligomer slightly more miscible with polystyrene than a cyclic. In any case, χ_{PS_L/PC_L} was not found to depend strongly on the nature of the end group (see Table 3), and more importantly, the difference between χ_{PS_L/PC_C} and χ_{PS_L/PC_L} is far too large to be due to the chemical nature of the end group.

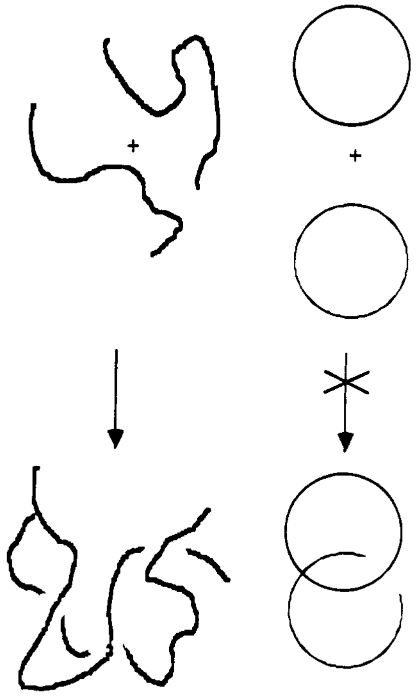

Figure 9. Schematic illustration of repulsive interactions between pairs of rings.

The following section describes the effect of topological constraints unique to ring polymers which results in $\chi_{PS_L/PC_C} < \chi_{PS_L/PC_L}$.

Phenomenological Model Rationalizing. $\chi_{PS_L/PC_C} < \chi_{PS_L/PC_L}$. Blends of cyclic polycarbonate oligomers with linear polystyrene have been shown to be miscible over a wider range of polystyrene molecular weights than corresponding linear oligomers. Although the Flory–Huggins theory is quite successful in predicting the shape of phase boundaries for both cyclic/linear and linear/linear blends, the interaction parameter depends strongly on topology. We assume that this topological dependence results from repulsive intermolecular interactions acting between rings that do not exist between linear chains or between rings and linears. This is illustrated schematically in Figure 9. If, as synthesized, two rings are not concatenated, they cannot exist in linked configurations in the condensed state. The necessary conservation of a system's topological state (i.e., presence or absence of linkages or concatenates) results in an additional topological excluded-volume interaction between ring polymers.[13,31] The origin of this interaction is the impenetrability of one cyclic molecule's core by another cyclic molecule core. This class of interaction does not occur between linear polymers which interpenetrate quite extensively and exhibit essentially no excluded volume to each other in the condensed state.[32]

Experimental evidence for a special topological interaction between ring molecules can be found in their dilute solution properties. The Flory θ temperature, at which the second virial coefficient vanishes, has been determined to be 6 °C lower for ring polystyrene than for linear polystyrene.[3,33,34] Thus, cyclic polymers display positive second virial coefficients at temperatures where the second virial coefficients for linear polymers are zero. This had been attributed to additional excluded-volume interactions which exist between cyclic polymers due to the topological constraints discussed above.[35−39]

Although there is general acceptance of the existence of unique topological interactions between cyclic polymers and an acceptance of their effect on dilute solution behavior, little attention has been paid to the possible significance of these interactions in the condensed state. Cates and Deutsch conjectured that topological constraints present in melts of cyclic polymers may lead to the following: (1) The partial collapse of ring polymers in the melt (i.e., rings may be non-Gaussian; $R_g \sim M^\nu$, $\nu = {}^2/_5$); (2) the swelling of rings in a melt of a chemically identical linear polymer, $\nu = {}^3/_5$; and (3) the enhancement of the thermodynamic stability of cyclic/linear blends of chemically dissimilar species relative to linear/linear blends.[13] The first two of these conjectures find support in results of computer simulations.[40,41]

In light of the above discussion, we present a simple phenomenological analysis to rationalize the inequality $\chi_{PS_L/PC_C} < \chi_{PS_L/PC_L}$. The model incorporates in a crude way the role of topological interactions between rings into the Flory–Huggins (FH) expression for the free energy of mixing and thus enables us to assess the separate effects of topology on the entropy and the energy of mixing. For definiteness, the random walk lattice language and notation of Hill[42] (three dimensional, simple cubic) is adopted. A polymer chain is modeled as a noninteracting nearest-neighbor random walk on a 3D Cartesian lattice with its first segment arbitrarily located at the origin (0,0,0). The fundamental quantity characterizing the walk is the conditional probability density $p_n(\mathbf{r})$ of finding the walker at the nth step (i.e., the $n + 1$ segment of the polymer) at position $\mathbf{r} = (x, y, z)$ on the lattice, assuming that the walker started at the origin. This quantity is known to be given by[43]

$$p_n(\mathbf{r}) = \frac{1}{(2\pi)^3}\int_{-\pi}^{\pi}\int_{-\pi}^{\pi}\int_{-\pi}^{\pi}\left[\frac{1}{3}(\cos\phi_1 + \cos\phi_2 + \cos\phi_3)\right]^n \exp(-i\phi\cdot\mathbf{r})\,d\phi \quad (11)$$

On a simple cubic 3D lattice, there are six different possible step directions (all of equal length) at each step of the walk, so there are altogether 6^n different walks (or polymer configurations) having exactly n steps. Equation 11 for $p_n(\mathbf{r})$ takes this total number of walks into account and enumerates that fraction of the 6^n that terminate precisely at $\mathbf{r}$.

Of course, polymer chains interact with themselves as well as with other chains, so that the random walk description contains several unrealistic features. Flory and Huggins modified the analysis in several simple ways. Instead of permitting a walker to immediately reverse its direction (and hence cause the ith segment to sometimes overlap the $i - 1$th, FH reduced the lattice coodination by 1 to approximately eliminate the effect of immediate reversals. Thus, if the original lattice had coordination Z, then in the FH method, at each step the walker has only $Z - 1$ choices for its next position. For a simple 3D cubic lattice, instead of 6^n total walks having n steps, one has 5^n.

Next, FH took prior occupancy of lattice sites into account by modifying the (already reduced) step-direction choices, $Z - 1$, by a factor that takes into account the average number of polymers already in place on the lattice. If the total number of available lattice sites is M_0, and if M is the degree of polymerization of the chains, then after j chains have been put on the lattice, the fraction of available (empty) sites is $\equiv 1 - jM/M_0$. Thus if ω_{j+1} equals the number of ways of putting the $j + 1$ polymer molecule on the lattice, the noninteracting random walk result

$$\omega_{j+1}^{RW} \equiv M_0 Z^M \quad (12)$$

becomes, in the FH approximation,

$$\omega_{j+1}^{FH} \cong M_0\left(1 - \frac{jM}{M_0}\right)[Z - 1]^{M-1}\left\{1 - \frac{jM}{M_0}\right\}^{M-1} \quad (13)$$

Using eq 13, one readily computes the entropy of mixing N_2 polymer molecules and N_1 solvent molecules on the M_0 lattice sites is

$$\Delta S_m/k = -N_1 \ln \theta_1 - N_2 \ln \theta_2 \quad (14)$$

where $\theta_1 = N_1/(N_1 + MN_2)$ is the site (i.e., volume) fraction of solvent and $\theta_2 = MN_2/(N_1 + MN_2)$ is the site fraction of polymer.

We attempt to extend the FH treatment of linear polymers to cyclic chains. Returning to eq 11, the probability that n step walks return to the origin (i.e., form loops) is given by

$$p_n(0) = \frac{1}{(2\pi)^3}\int_{-\pi}^{\pi}\int_{-\pi}^{\pi}\int_{-\pi}^{\pi}\left[\frac{1}{3}(\cos\phi_1 + \cos\phi_2 + \cos\phi_3)\right]^n d\phi \quad (15)$$

For moderately large n, this is approximately

$$p_n(0) \cong [6/n\pi]^{3/2} \quad (16)$$

which for $n = 10$, gives ~0.083 as the fraction of loops. For chains with 10 monomers (approximately the size of the oligomers used in this study) ~60 000 000 total random walks exist, of which ~5 000 000 form closed loops. It is this cyclic subset of the entire collection which we use to model cyclic PC molecules.

The constraint of forming a loop reduces the freedom of the random walker at each step, and we model the influence of this constraint (in a mean-field fashion) with an isotropically modified step probability. In the noninteracting case, the number of choices at each step is Z and now this becomes

$$Z \Rightarrow Z[6/M\pi]^{3/2M} \quad (17)$$

Thus after M steps one generates $Z^M[6/M\pi]^{3/2}$ total configurations and not Z^M as in the nonloop case. Equation 13, using the modified step probability of eq 17, leads again to eq 14 for the entropy of mixing N_1 solvent molecules and N_2 *cyclic* polymer molecules on M_0 sites, where now θ_2 is the site fraction of cyclic polymer chains. In this approximation, polymer topology has no effect on the entropy of mixing. A surprising result in light of the severe reduction in total chain configurations due to the step constraint (cf. eq 16), but understandable if the most probable location for the terminus of an n-step walk is at the origin, and the constraint restricts chain configurations to those that are favored in the absence of a constraint.[44] Turning to the effects on the *energy* of mixing, the mean-square radius of gyration, $\langle S^2\rangle$, of a cyclic molecule (or random walk) is smaller than that of the corresponding linear molecule:[45]

$$\langle S^2\rangle_{\text{cyclic}} = \frac{1}{12}nl^2 = \frac{1}{2}\langle S^2\rangle_{\text{linear}} \qquad (18)$$

This smaller size corresponds to a higher density, a higher probability of self-contacts, and a *reduced numbers of intermolecular contacts* with other cyclics. We assume that the probability of inter- and intramolecular contacts is proportional to the number fraction, f_{inter} and $f_{\text{intra}} = 1 - f_{\text{inter}}$, of each in the neighborhood of a given segment. From the larger single-chain segment densities of cyclics vs linears given by eq 18, on average one has

$$f_{\text{intra}}^{\text{cyclic}} = 2^{3/2} f_{\text{intra}}^{\text{linear}} \qquad (19)$$

so that self-contacts are 3 times more likely in a cyclic compared to a linear molecule of the same molecular weight. While it might seem that eq 19 becomes unimportant for large chains (i.e., $n > 100$, or so), since then the *fraction* of self-contacts is very low (less that 1%), it is the absolute number of self-contacts that is important for the cohesive energy and the majority of overlaps of a chain with itself happen locally. For the lattice model, Hill wrote for the cohesive energy of a polymer before mixing

$$E_{\text{cohesive}}^{\text{linear}} = MN_2(Z-2)w_{22} \qquad (20)$$

where $Z - 2$ is the "intermolecular" coordination of a lattice site, excluding the two bonded sites next to each non-end-group segment, MN_2 is the number of segments per chain times the number of chains, and w_{22} is the segment–segment contact energy of the polymer with itself. One may consider that either eq 20 ignors non nearest-neighbor contacts of the chain with itself (since these are infrequent for high molecular weights) or else it assumes that these have the same pair energy as segment interactions between different chains. In either case, the quantity w_{22} is comprised of two contributions (inter and intra), and the numbers of these differ for cyclic and linear polymers owing to the different self-contact densities (eq 19), and the noncrossing condition for cyclic molecules. We summarize this by writing

$$|(Z-2)w_{22}^{\text{linear}}| > |(Z-2)w_{22}^{\text{cyclic}}| \qquad (21)$$

and from eqs 2, 4, and 21 it follows that the different χ parameters for cyclic and linear PCs arise from the larger cohesive energy of the linear molecules.

One may note an additional example of the topological effect on mean-field interaction parameters. Hashimoto et al. studied the effect of arm number on the order–disorder transition of star–block copolymers.[46] Theoretical, disordered-state, SAXS profiles based on a mean-field random phase approximation fit experimental profiles quite well. However, the Flory–Huggins interaction parameter was found to depend strongly on the number of arms, n. χ decreased with increasing n; the largest drop coming between $n = 1$ and 2. This study in addition to our own reveals the sensitivity of the thermodynamics of mixing to the local structure of polymer melts. The details of local structure have been the focus of several recent theoretical developments.[47–49] Numerical results from Curro and Schweizer's integral equation approach also predict a negative interaction parameter for blends of chemically identical rings/linears. Unfortunately, the numerical methods required to solve the integral equations make it difficult to extract a simple physical mechanism for the final results.[47]

Summary

The thermodynamics of mixing has been shown to be quite sensitive to changes in the topology of blend components. Cyclic Bisphenol A carbonate cyclic oligomers are miscible with a wider range of polystyrene molecular weights than are chemically equivalent linear oligomers. The Flory–Huggins mean-field theory predicts the shape of phase boundaries quite well for linear polystyrene/linear polycarbonate blends as well as for linear polystyrene/cyclic polycarbonate blends. However, the interaction parameter was determined to be strongly dependent upon topology with $\chi_{\text{PS}_\text{L}/\text{PC}_\text{C}} < \chi_{\text{PS}_\text{L}/\text{PC}_\text{L}}$. This result has been explained in terms of a topological repulsion between ring polymers which is expected to be quite general. Small-angle neutron scattering studies are planned to confirm the partial collapse of ring polymers in the homogeneous melt as well as their swelling in blends with linear polymers (chemically equivalent as well as chemically dissimilar).

References and Notes

(1) Tead, S. F.; Kramer, E. J.; Hadziioannou, G.; Antonietti, M.; Sillescu, H.; Lutz, P.; Strazielle, C. *Macromolecules* **1992**, *25*, 3942.
(2) García Bernal, J. M.; Tirado, M. M.; Freire, J. J.; García, de la Torre, J. *Macromolecules* **1990**, *23*, 3357.
(3) McKenna, G. B.; Hostetter, B. J.; Hadjichristidis, N.; Fetters, L. J.; Plazek, D. J. *Macromolecules* **1989**, *22*, 1834.
(4) Mills, P. J.; Mayer, J. W.; Kramer, E. J.; Hadziioannou, G.; Lutz, P.; Strazielle, C.; Rempp, P.; Kovacs, A. J. *Macromolecules* **1987**, *20*, 513.
(5) McKenna, G. B.; Hadziioannou, G.; Lutz, P.; Hild, G.; Strazielle, C.; Straupe, C.; Rempp, P.; Kovacs, A. J. *Macromolecules* **1987**, *20*, 498.
(6) Hadziioannou, G.; Cotts, P. M.; ten Brinke, G.; Han, C.; Lutz, P.; Strazielle, C.; Rempp, P.; Kovacs, A. J. *Macromolecules* **1987**, *20*, 493.
(7) Utracki, L. A. *Polymer Alloys and Blends: Thermodynamics and Rheology*; Hanser: New York, 1989.
(8) Solc, K., Ed. *Polymer Compatibility and Incompatibility: Principles and Practices*; MMI: New York, 1982.
(9) Paul, D. R., Newman, S., Eds. *Polymer Blends*; Academic: New York, 1978; Vols. 1 and 2.
(10) Olabisi, O.; Robeson, L. M.; Shaw, M. T. *Polymer–Polymer Miscibility*; Academic: New York, 1979.
(11) Santore, M. M.; Han, C. C.; McKenna, G. B. *Macromolecules* **1992**, *25*, 3416.
(12) Faust, A. B.; Sremcich, P. S.; Gilmer, J. W.; Mays, J. W. *Macromolecules* **1989**, *22*, 1259.
(13) Cates, M. E.; Deutsch, J. M. *J. Phys.* **1986**, *47*, 2121.
(14) Brunelle, D. J.; Bowden, E. P.; Shannon, T. G. *J. Am. Chem. Soc.* **1990**, *117*, 2399.
(15) Brunelle, D. J.; Shannon, T. G. *Macromolecules* **1991**, *24*, 3035.
(16) Brunelle, D. J. In *Ring Opening Polymerization*; Brunelle, D. J., Ed.; Hanser Verlag: Munich, 1992; Chapter 11.
(17) Brunelle, D. J., personal communication.
(18) Yang, A. J.-M.; Di Marzio, E. A. *Macromolecules* **1991**, *24*, 6012, and references therein.
(19) Hay, A. S.; Williams, F. J.; Loucks, G. M.; Relles, H. M.; Boulette, B. M.; Donahue, P. E.; Johnson, D. S. *Polym. Prepr. (Am. Chem. Soc., Div. Polym. Chem.)* **1982**, *23* (2), 117.
(20) Koningsveld, R.; Staverman, A. J. *J. Polym. Sci., A-2* **1968**, *6*, 305.
(21) Koningsveld, R.; Staverman, A. J. *J. Polym. Sci., A-2* **1968**, *6*, 325.
(22) Koningsveld, R.; Staverman, A. J. *J. Polym. Sci., A-2* **1968**, *6*, 349.
(23) Koningsveld, R.; Kleintjens, L. A. *J. Polym. Sci., Polym. Symp.* **1977**, *61*, 221.
(24) Solc, K. *Macromolecules* **1970**, *3*, 665.
(25) Casassa, E. F. *J. Polym. Sci., Polym. Symp.* **1976**, *54*, 53.

(26) Han, C. C.; Bauer, B. J.; Clark, J. C.; Muroga, Y.; Matsushita, Y.; Okada, M.; Tran-Cong, Q.; Chang, T.; Sanchez, I. C. *Polymer* **1988**, *29*, 2002.

(27) Flory, P. J. *Discuss. Faraday Soc.* **1970**, *49*, 7.

(28) For details see: (a) *Polymer User Guide Pt. 2*, version R-5.0; Biosym Technologies: San Diego, CA, 1992. (b) Qian, C.; Mumby, S. J.; Eichinger, B. E. *Polym. Prepr. (Am. Chem. Soc., Div. Polym. Chem.)* **1990**, *31* (2), 691. (c) Mumby, S. J.; Sher, P. B.; Eichinger, B. E. *Polymer*, in press.

(29) Kim, W. N.; Burns, C. M. *J. Appl. Polym. Sci.* **1987**, *34*, 945.

(30) Callaghan, T. A. Ph.D. Dissertation: U. Texas, Austin, TX 1992 (with D. R. Paul).

(31) (a) Frank-Kamenetskii, M. D.; Lukashin, A. V.; Vologodskii, A. V. *Nature* **1975**, *258*, 398. (b) des Cloizeaux, J.; Mehta, M. L. *J. Phys.* **1979**, *40*, 665.

(32) de Gennes, P. G. *Scaling Concepts in Polymer Physics*; Cornell University Press: Ithaca, NY, 1979.

(33) Roovers, J.; Toporowski, P. M. *Macromolecules* **1983**, *16*, 843.

(34) Roovers, J. *J. Polym. Sci., Polym. Phys.* **1985**, *23*, 1117.

(35) Casassa, E. F. *J. Polym. Sci., Part A* **1965**, *3*, 605.

(36) Tanaka, F. *J. Chem. Phys.* **1987**, *87*, 4201.

(37) Iwata, K. *Macromolecules* **1985**, *18*, 116.

(38) Iwata, K.; Kimura, T. *J. Chem. Phys.* **1981**, *74*, 2039.

(39) des Cloizeaux, J. *J. Phys.-Lett.* **1981**, *42*, L-433.

(40) Pakula, T.; Geyler, S. *Macromolecules* **1988**, *21*, 1665.

(41) Geyler, S.; Pakula, T. *Makromol. Chem., Rapid Commun.* **1988**, *9*, 617.

(42) Hill, T. L. *An Introduction to Statistical Mechanics*; Addison Wesley: Reading, MA, 1960; Chapter 21.

(43) Montroll, E. W. *Proc. Symp. Appl. Math.* **1964**, *16*, 193.

(44) Weiss, G. H. *Aspects and Applications of the Random Walk*; North Holland: New York, 1994; Chapter 4.

(45) Yamakawa, H. *Modern Theory of Polymer Solutions*; Harper and Row: New York, 1971; p 322.

(46) Ijichi, Y.; Hashimoto, T.; Fetters, L. J. *Macromolecules* **1989**, *22*, 2817.

(47) Curro, J. G.; Schweizer, K. S. *Macromolecules* **1990**, *23*, 1402.

(48) Pesci, A. I.; Freed, K. F. *J. Chem. Phys.* **1989**, *90*, 2017.

(49) Muthukumar, M. *J. Chem. Phys.* **1986**, *89*, 4722.

MA946403Z